AGU ADVANCING EARTH AND SPACE SCIENCES

Geophysical Research Letters

RESEARCH LETTER
10.1029/2024GL112562

Source Limitation Could Have Major Implications to Dust Emission Estimates

Yaping Shao[1], **Siyu Chen**[2], **Ning Huang**[3], **Hailin Gui**[4], **Rui Mao**[5], **Ishizuka Masahide**[6], **Chenglai Wu**[7], **Xin Yin**[5], **and Jie Zhang**[3]

[1]Institute for Geophysics and Meteorology, University of Cologne, Köln, Germany, [2]Department of Atmospheric Sciences, Lanzhou University, Gansu, China, [3]College of Civil Engineering and Mechanics, Lanzhou University, Gansu, China, [4]National Meteorological Center, Chinese Meteorological Administration, Beijing, China, [5]School of National Safety and Emergency Management, Beijing Normal University, Beijing, China, [6]Department of Engineering and Design, Kagawa University, Kagawa, Japan, [7]Institute for Atmospheric Physics, Chinese Academy of Sciences, Beijing, China

Key Points:

- A new model for source-limited dust emission is proposed
- Impact of source limitation to dust emission is profound and model predicted dust emission can reduce by order of magnitude
- Global dust model estimated dust emission may be a substantial overestimate

Supporting Information:

Supporting Information may be found in the online version of this article.

Correspondence to:

J. Zhang,
zhang-j@lzu.edu.cn

Citation:

Shao, Y., Chen, S., Huang, N., Gui, H., Mao, R., Masahide, I., et al. (2025). Source limitation could have major implications to dust emission estimates. *Geophysical Research Letters*, *52*, e2024GL112562. https://doi.org/10.1029/2024GL112562

Received 20 SEP 2024
Accepted 16 DEC 2024

Author Contributions:

Conceptualization: Yaping Shao, Siyu Chen, Chenglai Wu, Jie Zhang
Data curation: Ishizuka Masahide
Formal analysis: Yaping Shao
Funding acquisition: Ning Huang, Jie Zhang
Methodology: Yaping Shao, Siyu Chen, Hailin Gui, Rui Mao, Chenglai Wu, Xin Yin
Project administration: Ning Huang, Jie Zhang
Software: Yaping Shao, Hailin Gui, Rui Mao, Xin Yin
Validation: Yaping Shao
Visualization: Yaping Shao, Ishizuka Masahide
Writing – original draft: Yaping Shao
Writing – review & editing: Rui Mao

Abstract

A model for source-limited dust emission is proposed. The model accounts for the evolution of the supply of soil dust depleted by dust emission and enriched by the process of surface renewal, together with several other new developments. The model is tested with a field dataset. The impact of source limitation to dust emission is profound. Our tests show that by considering source limitation, the model predicted dust emission can reduce by one order of magnitude in a real-case simulation period of less than 20 days. We show that the process of dust emission is much more complex and variable than considered in previous dust models. Our findings have far-reaching implications, for example, to the global dust emission estimates. Because source-limited dust emission has so far not been represented in global dust models, the model estimated dust emission is only its potential and may be a substantial overestimate.

Plain Language Summary

Airborne dust is important to climate change. Models exist to estimate how much dust is emitted from the surface every year. But these models do not account for source limited dust emission. This lack of capacity may cause serious errors in the estimated dust emission. Here, we develop a new model to overcome this problem, which simulates the evolution of dust availability on the surface. We test our model using observed data and found that the impact of source limited dust emission is very large. This is the first source-limited dust emission model we know. Our findings have far-reaching implications to climate research. We believe that existing global dust emission estimates may be too large.

1. Introduction

Are global dust emission estimates reliable? In recent decades, these estimates have been repeatedly revised from 500 to 3,000 (Shao et al., 2011) to 1,000–4,000 (Boucher et al., 2013) and to 5,000 Tg yr^{-1} (Kok et al., 2021). A serious deficit of the existing dust models is their incapacity in modeling source-limited dust emission (SLDE) (Webb et al., 2021). Two types SLDE exist. First, factors such as surface cover, soil moisture, surface crust etc. limit dust emission by influencing wind erosion dynamics. In dust models, these factors are reflected in the threshold friction velocity u_{*t} for wind erosion:

$$u_{*t}(d;\theta,\lambda,s,c\ldots) = u_{*t0}(d)f_\theta(\theta)f_\lambda(\lambda)f_s(s)f_c(c)\ldots \tag{1}$$

where d is particle size, θ soil moisture, λ surface roughness density, s soil salt content, and c surface crust; u_{*t0} is the threshold friction velocity for an idealized surface and $f_\theta(\theta)$, $f_\lambda(\lambda)$ etc. are modification functions accounting for the effects of soil moisture, surface roughness etc., respectively. Schemes for $u_{*t0}(d)$ have been proposed (Bagnold, 1941; Shao & Lu, 2000) and various modification functions, for example, by Fécan et al. (1999) for $f_\theta(\theta)$. While large uncertainties exist in modeling u_{*t}, for example, in quantifying the effect of surface crust, we have conceptually considered the first type SLDE in dust models and know the challenges. Second, SLDE occurs if the parent soil has a limited supply of dust for emission or is depleted of dust due to emission. Here, we study the second type SLDE. Figure 1a depicts the evolution of soil particle size distributions (PSDs), one before and the other after a dust event. In the latter case, because of dust emission, the topsoil is depleted of dust and becomes sandier and the availability of dust for emission becomes limited. On the other hand, the topsoil can be enriched of dust via surface renewal and weathering processes. Surface renewal is a process which replenishes the amount of

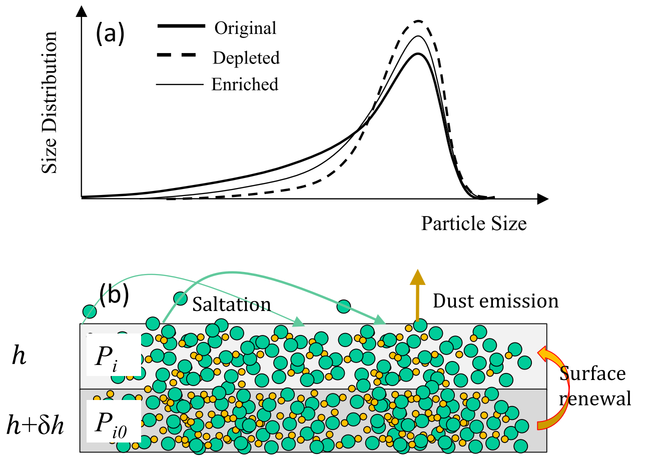

Figure 1. (a) Illustration of soil PSD evolution. Depicted are the soil PSDs before a dust event (original), depleted of dust due to dust emission (depleted) and enriched by surface renewal and weathering (enriched). (b) Illustration of the processes related to SLDE. The depth of the erodible soil layer h is assumed to be proportional to streamwise saltation flux Q. An increase in Q leads to an increase of h to $h + \delta h$, mixing dust from a deep soil layer, for which the mass fraction of dust bin i is P_{i0}, to the topsoil layer, for which the mass fraction of dust bin i is P_i.

surface dust by saltation mixing of soil particles (Zhang et al., 2016). Weathering processes on various time scales can modify soil PSD and increase the supply of dust for emission, for example, alluvial dust deposits in river beds are important local dust sources and biogeochemical processes in desert areas may influence the availability of dust for emission on climate time scales.

The lack of capacity for modelling SLDE has serious implications to global climate research and dust weather forecast. As global dust models only predict the potential dust emission under unlimited supply, the estimates of the global dust emission are probably larger than that in reality, leading to errors in the estimates of aerosol radiative forcing. For weather forecasts, this lack may result in false alarms or wrong intensity estimates of dust storms.

As Figure 1a implies, to account for SLDE requires modelling the evolution of soil PSD and needs to be based on schemes which can model size-resolved dust emission fluxes. Several such schemes exist (Klose et al., 2021; Kok et al., 2014; LeGrand et al., 2019; Shao, 2004). Here, we present a new SLDE model, carry out numerical experiments with it and discuss the implications of SLDE.

2. Source-Limited Dust Emission Model

2.1. Dynamic Evolution of Soil Particle Size Distribution

Consider a unit area of soil and suppose the depth of the erodible soil layer is h. Then, the total mass of the erodible soil m is

$$m = \rho_s h \tag{2}$$

where ρ_s is bulk soil density. Suppose the erodible soil has a PSD $p(d)$ and the full particle-size range is divided into N bins, with bin i of width Δd_i centered at d_i. Then, the erodible soil mass for bin i is

$$m_i = m \cdot P_i \tag{3}$$

where $P_i = p(d_i)\Delta d_i$ is the mass fraction of bin i. The derivative of Equation 3 after time gives

$$\frac{d \ln P_i}{dt} = -\frac{d \ln m}{dt} + \frac{d \ln m_i}{dt} \tag{4}$$

Suppose the dust emission rate from bin i is F_i, and that, due to surface renewal, soil from deeper layers is mixed into the erosion layer and P_{i0} is the mass fraction for bin i of the renewed soil (Figure 1b). Then, we have

$$\frac{1}{m_i}\frac{dm_i}{dt} = -\frac{F_i}{m_i} + \frac{1}{m}\frac{dm}{dt}\frac{P_{i0}}{P_i} \tag{5}$$

From Equation 2, we have

$$\frac{1}{m}\frac{dm}{dt} = \frac{1}{\rho_s h}\frac{d\,\rho_s h}{dt} - \frac{\sum F_i}{m} \tag{6}$$

The last term is the loss of total erodible soil mass due to dust emission, which we shall neglect. Substituting Equations 5 and 6 into Equation 4 gives

$$\frac{d \ln P_i}{dt} = -\frac{d \ln h}{dt}\left(1 - \frac{P_{i0}}{P_i}\right) - \frac{F_i}{m_i} \tag{7}$$

A finite-difference form of Equation 7 is

$$\ln P_i(t+\Delta t) - \ln P_i(t) = -[\ln h(t+\Delta t) - \ln h(t)] \cdot \left(1 - \frac{P_{i0}}{P_i}\right) - \frac{F_i}{m_i}\Delta t \tag{8}$$

Equation 8 shows two mechanisms drive the evolution of $P_i(t)$. First, a net dust emission ($F_i > 0$) leads to a reduction of P_i. Second, the surface renewal process, that is, an increase in h with $P_{i0} \neq P_i$, leads to a change of P_i and with $P_{i0} > P_i$, a restoration of particles of size d_i for dust emission.

Like a creep layer (Wang et al., 2020), we assume h and Q are linearly related,

$$h = a_h Q \tag{9}$$

with a_h being a coefficient. Using Equation 9, we rewrite Equation 8 as

$$\ln P_i(t+\Delta t) - \ln P_i(t) = -\epsilon_r[\ln Q(t+\Delta t) - \ln Q(t)] \cdot \left(1 - \frac{P_{i0}}{P_i}\right) - \frac{F_i}{m_i}\Delta t \tag{10}$$

where ϵ_r represents the degree of soil mixing in the erodible soil layer. For $\epsilon_r = 0$, surface renewal has no impact, while for $\epsilon_r = 1$, its full impact on the PSD of the erodible soil layer. In Equation 10, a_h does not explicitly appear but is used to compute $h + \delta h$, which P_{i0} is associated with.

Weathering modifies the soil PSD, which involves numerous environment factors, such as solar radiation, temperature, rainfall, and other bio-geochemical variables. A full weathering model is not our purpose, and a simple representation of the weathering effect is to assume that

$$\frac{\mathrm{d}m_{\mathrm{i}}}{dt} = r_i m_i + c_i \tag{11}$$

with r_i being the weathering rate and c_i a source term due to factors such as deposition, alluvial and freezing-and-throwing processes. Equation 10 can now be written as

$$\ln P_i(t+\Delta t) - \ln P_i(t) = -\epsilon_r[\ln Q(t+\Delta t) - \ln Q(t)] \cdot \left(1 - \frac{P_{i0}}{P_i}\right) - \left(\frac{F_i}{m_i} - r_i - \frac{c_i}{m_i}\right)\Delta t \tag{12}$$

Numerically, the term $\frac{P_{i0}}{P_i}$ is problematic if P_i is small. We thus solve Equation 12 in two steps. In step 1, we solve for surface renewal

$$\frac{d \ln P_i}{dt} = -\epsilon_r \frac{d \ln Q}{dt}\left(1 - \frac{P_{i0}}{P_i}\right) \tag{13}$$

which can be written as

$$\frac{dP_i}{dt} = -\epsilon_r \frac{d \ln Q}{dt}(P_i - P_{i0}) \tag{14}$$

An interim P_i, denoted as P_i^*, is computed

$$P_i^* = P_i + \epsilon_r (P_{i0} - P_i) \ln\left(\frac{Q(t+\Delta t)}{Q(t)}\right) \tag{15}$$

In step 2, we solve for dust depletion/weathering

$$\frac{d \ln P_i}{dt} = -\left(\frac{F_i}{m_i} - r_i - \frac{c_i}{m_i}\right) \tag{16}$$

which gives

$$P_i(t+\Delta t) = P_i^* \cdot \exp\left[-\left(\frac{F_i}{m_i} - r_i - \frac{c_i}{m_i}\right)\Delta t\right] \tag{17}$$

Equation 12 shows that equilibrium states of SLDE are possible. In short-term, dust production by weathering can be neglected and a quasi-equilibrium is achieved if

$$\frac{F_i}{m_i}\Delta t = -\epsilon_r[\ln Q(t+\Delta t) - \ln Q(t)/Q(t)] \cdot \left(1 - \frac{P_{i0}}{P_i}\right)$$

This state is not steady, because P_{i0} drops overtime to P_i and F_i drops to zero. In long-term, $P_{i0} = P_i$ is expected and an equilibrium is achieved with

$$\frac{F_i}{m_i} = r_i + \frac{c_i}{m_i}$$

implying that long-term dust emission is constrained by weathering processes, as is probably the case in today's climate.

2.2. Model for Saltation and Dust Emission Fluxes

In addition to SLDE, the dust model includes two novel developments. One, the Shao (2004) scheme for saltation-bombardment and aggregates-disintegration (SBAD) dust emission is combined with the Klose and Shao (2012) scheme. The latter, originally designed for convective turbulence dust emission, is generalized for aerodynamic dust emission. Two, the turbulent nature of saltation and dust emission is considered by treating both friction velocity u_* and threshold friction velocity u_{*t} as stochastic variables. The model is summarized in Figure S1 and detailed in Supporting Information S1.

3. Example of Model Application

3.1. Idealized Experiment

An idealized test is done by assuming the atmospheric surface layer is neutral with $u_* = 0.4$ m·s^{-1}, $\rho = 1.23$ kg·m^{-3}, $\theta = 0.0$ m^3·m^{-3}, and fraction of surface cover $\sigma = 0.0$. The surface renewal process is excluded. The minimally and fully dispersed soil PSDs, $p_m(d)$ and $p_f(d)$, are specified for loam sand. Figure 2a shows that the simulated dust emission rate F decreases with time from about 20,000 μg·m^{-2} s^{-1} at the start to less than 5,000 μg·m^{-2} s^{-1} at the end of the simulation of about 20 days, while the streamwise saltation flux Q increases with time and approaches an equilibrium at ∼34 g·m^{-1} s^{-1}. The decrease in F is caused by the dust depletion due to emission, and the increase in Q as the soil texture coarsens. Also plotted is F/Q, the saltation bombardment efficiency, which decreases substantially with time as the soil becomes sandier.

An example for the evolutions of $p_m(d)$ and $p_f(d)$, together with the sediment PSD $p_s(d)$, is shown in Figure 2b. After 2 days of continuous dust emission, the amount of dust both in $p_m(d)$ and $p_f(d)$ are depleted, which in turn results in the reduced amount of dust in $p_s(d)$ and limits the dust emission rate as seen in Figure 2a.

3.2. Real Case Experiment

The data of the Japan-Australian Dust Experiment (JADE) are used to drive the dust model and for comparison. The JADE dataset, outlined in Supporting Information S2, has been used before (Alfaro et al., 2022). We carried out four groups of experiments using the JADE data (Supporting Information S2). Exp0 is the reference run with no SLDE, Exp1 is with SLDE but no surface renewal and Exp2 is as Exp1, but with surface renewal. Exp3, as Exp2 but with weathering (not sown).

Figure 3 compares the dust fluxes F_{exp0}, F_{exp1} and F_{exp2} for Exp0, Exp1 and Exp2, respectively. Figure 3a shows F_{exp0} as reference and Figure 3b the relative differences, for example, $\Delta F/F_{\mathrm{exp0}} \equiv (F_{\mathrm{exp0}} - F_{\mathrm{exp1}})/F_{\mathrm{exp0}}$, for Exp1 and Exp2. For all three runs, the predicted dust fluxes vary over many orders of magnitude but are

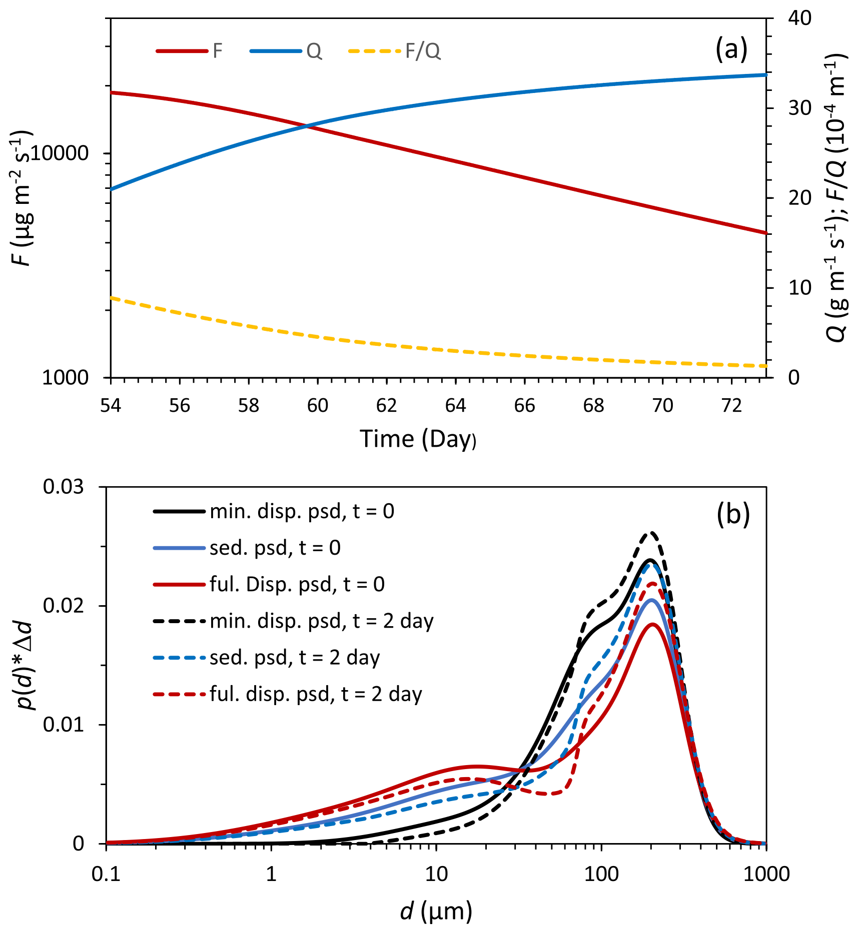

Figure 2. (a) Streamwise saltation flux Q and dust emission rate F for the idealized experiment. (b) Evolution of minimally, fully dispersed and sediment PSDs [in dust bin mass fraction $p_m(d)\Delta d$, $p_f(d)\Delta d$] and $p_s(d)\Delta d$] at time zero and 2 days.

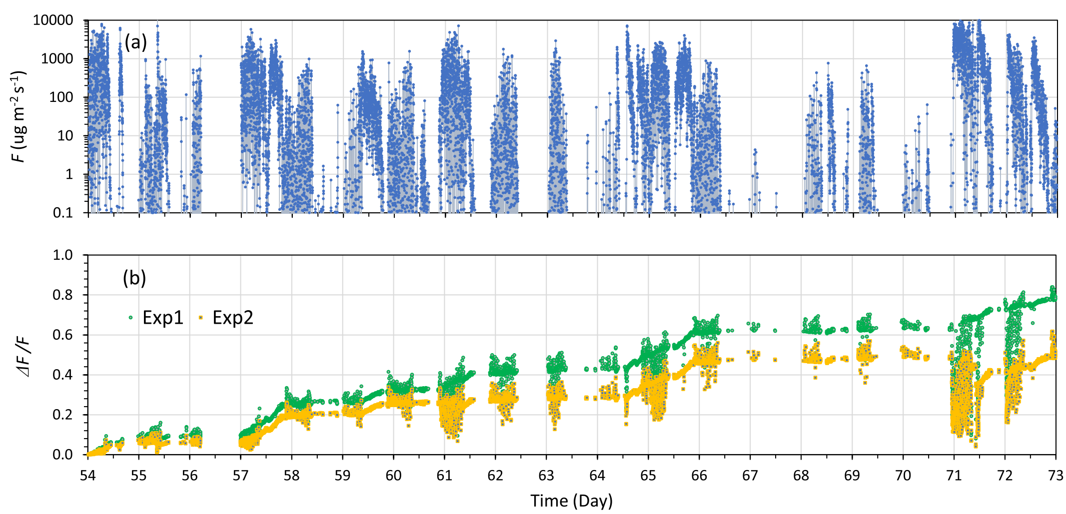

Figure 3. (a) For Exp0, simulated dust flux F_{exp0} in $\mu g{\cdot}m^{-2}\,s^{-1}$ for the JADE period; (b) relative differences of F_{exp1} and F_{exp2} with respect to F_{exp0}.

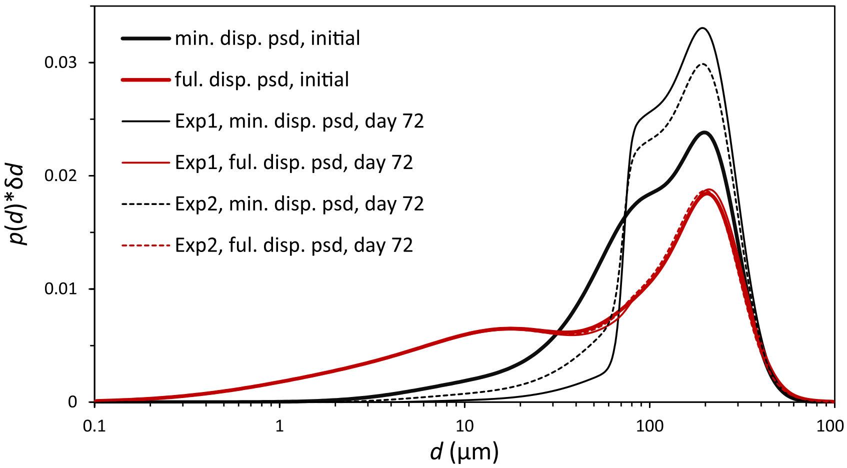

Figure 4. Initial minimally (black lines) and fully dispersed (red lines) soil PSDs and the simulated ones for JADE Day 72 for Exp1 (SLDE with no surface renewal) and Exp2 (SLDE with surface renewal).

qualitative similar. The frequent occurrence of the weak dust fluxes is attributed to both weak SBAD and aerodynamic dust emission. Figure 3b shows that the relative differences between F_{exp0}, F_{exp1} and F_{exp2} are initially small as the soil PSDs for all three runs are similar. As time increases, the differences between them increase due to the evolution of the soil PSDs. Between them, F_{exp0} is the largest and F_{exp1} the smallest, because for Exp0, dust depletion is not accounted for, while for Exp1 the soil PSDs evolve, and soil dust is depleted by dust emission. F_{exp2} falls between F_{exp0} and F_{exp1} because the depleted soil dust is partially compensated by surface renewal. Figure 3b shows, by the end of the simulation, F_{exp1} is less than $0.2F_{\mathrm{exp0}}$, and F_{exp2} less than $0.5F_{\mathrm{exp0}}$. For a longer simulation period, the differences between these fluxes will be even larger, because F_{exp1} will approach zero when soil continues to be depleted of dust.

As Equation S13 in Supporting Information S1 describes, γ fraction of the SBAD dust emission originates from the free dust, represented using the minimally dispersed PSD, and $(1-\gamma)$ fraction from aggregated dust, represented using the fully dispersed PSD. Thus, the PSDs $p_m(d)$, $p_f(d)$ and $p_s(d)$ all evolve with time. For Exp0, $p_m(d)$ and $p_f(d)$ do not change with time. Figure 4 compares for Exp1 and Exp2 the averaged $p_m(d)$ and $p_f(d)$ on JADE Day 72 with their initial specifications. With no surface renewal (Exp1), as seen in $p_m(d)$, dust particles are significantly depleted, but in $p_f(d)$, a considerable amount of aggregated dust still exists. This is because aggregated dust is emitted mainly under strong wind conditions. Figure 3c shows that u_* during JADE was not excessively large, mostly below 0.4 $\mathrm{m \cdot s^{-1}}$ apart from Day 71. Thus, the depletion of the aggregated dust occurs at a much slower rate than that of the free dust. In comparison, as Exp2 shows, the surface renewal process can compensate the depletion of dust by making dust from deeper soil layers available for emission.

A comparison between the modeled and observed dust emissions is made. In JADE, the emission rate for dust particles smaller than 12 μm (PM12) was estimated from the dust concentration profile measurements, which we denote as F_{12}. As our model predicts size-resolved dust fluxes, F_{12} can be calculated from the model output. Figure 5 shows the comparison of F_{12} simulated in Exp0 and Exp1 and observed in JADE. The model reproduces the observed dust emission to the correct order of magnitude (Figure 5a). For the initial phase (Figure 5b), F_{12} simulated in Exp0 and Exp1 are very similar and close to the JADE observations, except for the period 53.6–54.2 days. In the end phase (Figure 5c), due to the evolution of the soil PSDs, F_{12} simulated in Exp0 and Exp1 differ significantly, with Exp0 predicting larger values and Exp1 smaller. Toward the end of the simulation, Exp1 provides a better agreement with the JADE data.

For quantitative comparison, we calculate the accumulative sand drift D_{J}, dust emission E_{J} and PM12 emission $E_{12\mathrm{J}}$ over the JADE period, defined respectively as

$$D_{\mathrm{J}} = \int_{JADE} Q \cdot dt; \;\; E_{\mathrm{J}} = \int_{JADE} F \cdot dt; \;\; E_{\mathrm{J}12} = \int_{JADE} F_{12} \cdot dt$$

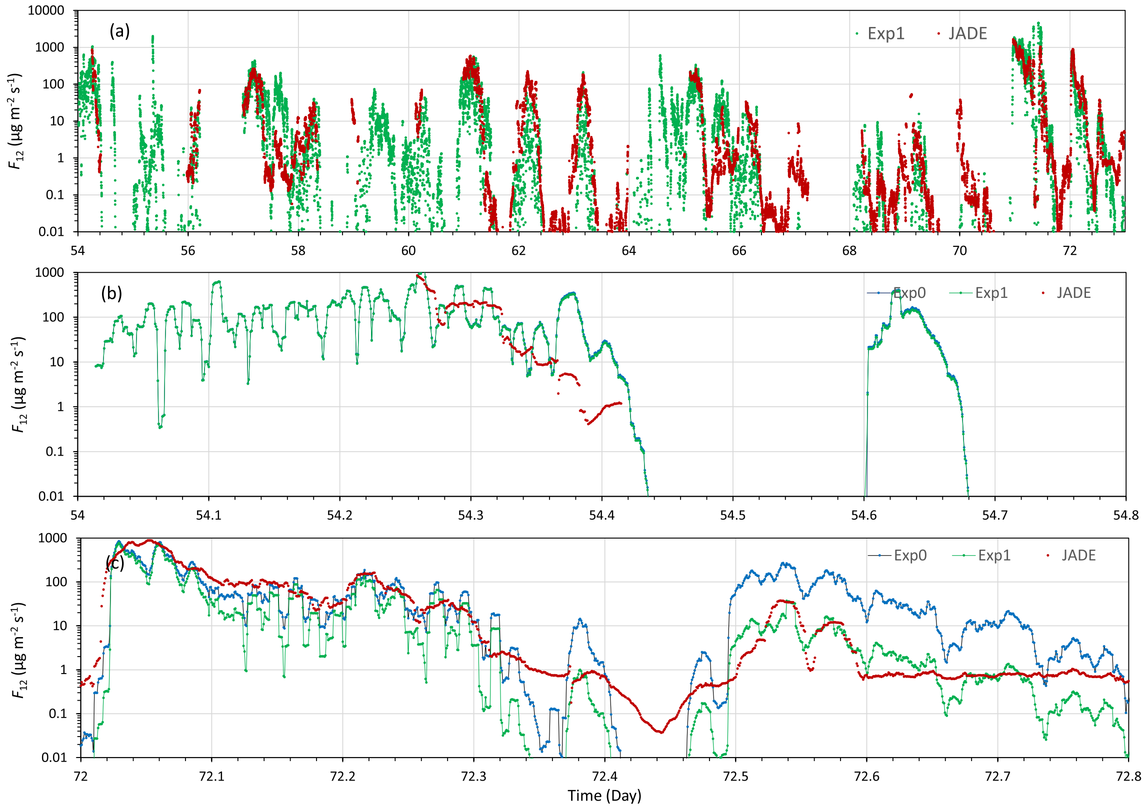

Figure 5. (a) Comparison of Exp1-simulated with JADE-observed PM12 emission rate F_{12}; (b) As (a), with Exp0 added, but for the initial period of JADE, here set to 54.0–54.8 days; and (c) As (b), but for the final phase of JADE, here set to 72.0–72.8 days.

These values are listed Table 1 together with the ratios E_J/D_J and E_{J12}/D_J. Again, the smallest D_J and largest E_J and E_{J12} are predicted for Exp0, while the largest D_J and smallest E_J and E_{J12} are predicted for Exp1. E_J and E_{J12} for Exp1 are ~70% and ~85% of those for Exp0. This implies that, in the period of 20 days, the accumulative dust emission is reduced by 30% and the accumulative PM12 emission is reduced by 15%. Over a longer period, the reduction in dust emission will be even more pronounced as dust depletion continues by dust emission. The increased sand drift and reduced dust emission for Exp1 with respect to Exp0 imply that the saltation bombardment efficiencies E_J/D_J and E_{J12}/D_J are smaller for Exp1 than for Exp0. The values of D_J, E_J and E_{J12} for Exp2 fall between those for Exp0 and Exp1. For a short time periods (e.g., days), surface renewal process can partially compensate the dust depletion by dust emission, but for long time periods (e.g., years), if the weathering process for dust generation is neglected, as the deep soil layer is also depleted of dust, the effect of surface renewal will be less important or even counterproductive. Suppose in Equation 9 $a_h = 0.5$ s·kg^{-1}, then a $Q = 10$ g·m^{-1} s^{-1} corresponds to $h = 5$ mm. The parameter a_h is not yet well known and varies in space and time, we conducted a sensitivity test in Supporting Information S2 A smaller a_h implies that a shallower soil layer can be renewed, and dust emission is more strongly source limited and vice versa.

Table 1
Comparison of Exp0-, Exp1- And Exp2-Simulated Accumulative Sand Drift D_J, Dust Emission E_J and PM12 Dust Emission E_{J12} for the JADE Period

	D_J (kg m^{-1})	E_J (g m^{-2})	E_{J12} (g m^{-2})	E_J/D_J (m^{-1})	E_{J12}/D_J (m^{-1})
Exp0	309	278	67	0.00090	0.00022
Exp1 (Exp1/Exp0)	366 (1.18)	194 (0.70)	57 (0.85)	0.00053	0.00016
Exp2 (Exp2/Exp0)	350 (1.13)	224 (0.81)	60 (0.90)	0.00064	0.00017

Note. Also shown are bombardment efficiencies E_J/D_J and E_{J12}/D_J.

4. Summary

We proposed a SLDE scheme by modeling the evolution of soil PSD, in which the three processes affecting soil PSD were considered, including dust depletion by dust emission, surface renewal and weathering. Idealized and real-case model runs with reference to observed data were carried out. We found that the evolution of soil PSD can strongly reduce the dust emission rate, depending on the length of the simulation period. Our findings have far-reaching implications to dust emission estimates. Because SLDE is so far not accounted for, global dust models only predict the potential of dust emission and likely substantially overestimate the real dust emission. It is common for global dust modeling to constrain the simulated atmospheric dust load using satellite data, but this technique is insufficient to constrain the dust budget, that is, the atmospheric dust load can be forced to agree with the satellite data for the wrong reason.

We demonstrated that the dynamics of dust emission is much more complicated than considered in previous dust models, because the surface renewal process is related not only to saltation but also to the vertical structure of the erodible soil layer. In short term, for a shallow erodible soil layer, dust for emission would be quickly depleted and dust emission reduced to small values (e.g., Gobi surface), while for a deep erodible soil layer (e.g., farmland), dust for emission could be enriched via the dust supply from deep soils and dust emission could stay for a considerable period at the potential level. In long term, the evolution of soil horizon due to sediment transport can have a marked effect on dust emission potential. Closer integration is thus required of dust, land-surface and ecosystem/carbon-cycle modeling.

We classified SLDE into first and second type, studied here the latter but did not consider all other important SLDE factors, for example, physical, chemical and biogenic soil crust. SLDE of all types need to be more comprehensively studied. Specific to this work, three issues require future research. One is to obtain observations to rigorously test the SLDE model; two is to critically examine the uncertainties in the existing (especially global) dust models, caused by their incapabilities in dealing with SLDE; and three is to establish a PSD database which SLDE modeling relies upon. Fortunately, thousands of soil samples are being collected worldwide and we are hopeful that such a database will become available soon.

Data Availability Statement

The JADE data used for model test are available from Ishizuka et al. (2021).

Acknowledgments
This research was funded by the National Key Research and Development Program (2023YFF1304203) and the National Natural Science Foundation of China (42376232). Open Access funding enabled and organized by Projekt DEAL.

References

Alfaro, S. C., Bouet, C., Khalfallah, B., Shao, Y., Ishizuka, M., Labiadh, M., et al. (2022). Unraveling the roles of saltation bombardment and atmospheric instability on magnitude and size distribution of dust emission fluxes: Lessons from the JADE and WIND-O-V experiments. *Journal of Geophysical Research: Atmospheres*, *127*(12). https://doi.org/10.1029/2021JD035983

Bagnold, R. A. (1941). *The physics of blown sand and desert dunes*. Methuen.

Boucher, O., Randall, D., & Artaxo, P. (2013). Clouds and aerosols. In T. F. Stocker, D. Qin, G. K. Plattner, et al. (Eds.), *Climate change 2013: The physical basis. Contribution of working group I to the fifth assessment report of the intergovernmental panel on climate change* (pp. 571–632). Cambridge University Press.

Fécan, F., Marticorena, B., & Bergametti, G. (1999). Parametrization of the increase of the aeolian erosion threshold wind friction velocity due to soil moisture for arid and semi-arid areas. *Annales Geophysicae*, *17*(1), 149–157. https://doi.org/10.1007/s00585-999-0149-7

Ishizuka, M., Mikami, M., Leys, J., & Shao, Y. (2021). JADE data 2 (Version 1). *Mendeley Data*. [Dataset]. https://doi.org/10.17632/pkvsms7ktn.1

Klose, M., Jorba, O., Gonçalves Ageitos, M., Escribano, J., Dawson, M. L., Obiso, V., et al. (2021). Mineral dust cycle in the multiscale online nonhydrostatic atmosphere chemistry model (MONARCH) version 2.0. *Geoscientific Model Development*, *14*(10), 6403–6444. https://doi.org/10.5194/gmd-14-6403-2021

Klose, M., & Shao, Y. (2012). Stochastic parameterization of dust emission and application to convective atmospheric conditions. *Atmospheric Chemistry and Physics*, *12*(16), 7309–7320. https://doi.org/10.5194/acp-12-7309-2012

Kok, J. F., Adebiyi, A. A., Albani, S., Balkanski, Y., Checa-Garcia, R., Chin, M., et al. (2021). Improved representation of the global dust cycle using observational constraints on dust properties and abundance. *Atmospheric Chemistry and Physics*, *21*(10), 8127–8167. https://doi.org/10.5194/acp-21-8127-2021

Kok, J. F., Mahowald, N. M., Fratini, G., Gillies, J. A., Ishizuka, M., Leys, J. F., et al. (2014). An improved dust emission model – Part 1: Model description and comparison against measurements. *Atmospheric Chemistry and Physics*, *14*(23), 13023–13041. https://doi.org/10.5194/acp-14-13023-2014

LeGrand, S. L., Polashenski, C., Letcher, T. W., Creighton, G. A., Peckham, S. E., & Cetola, J. D. (2019). The AFWA dust emission scheme for the GOCART aerosol model in WRF-Chem v3.8.1. *Geoscientific Model Development*, *12*(1), 131–166. https://doi.org/10.5194/gmd-12-131-2019

Shao, Y. (2004). Simplification of a dust emission scheme and comparison with data. *Jounal of Geophysical Research*, *109*(10), D10202. https://doi.org/10.1029/2003JD004372

Shao, Y., & Lu, H. (2000). A simple expression for wind erosion threshold friction velocity. *Journal of Geophysical Research*, *105*(D17), 22437–22444. https://doi.org/10.1029/2000JD900304

Shao, Y., Wyrwoll, K.-H., Chappell, A., Huang, J., Lin, Z., McTainsh, G. H., et al. (2011). Dust cycle: An emerging core theme in Earth system science. *Aeolian Research*, *2*(4), 181–204. https://doi.org/10.1016/j.aeolia.2011.02.001

Wang, P., Zhang, J., Dun, H., Herrmann, H. J., & Huang, N. (2020). Aeolian creep transport: Theory and experiment. *Geophysical Research Letters*, *47*(15), e2020GL088644. https://doi.org/10.1029/2020GL088644

Webb, N. P., LeGrand, S. L., Cooper, B. F., Courtright, E. M., Edwards, B. L., Felt, C., et al. (2021). Size distribution of mineral dust emissions from sparsely vegetated and supply-limited dryland soils. *Journal of Geophysical Research: Atmospheres*, *126*(22), e2021JD035478. https://doi.org/10.1029/2021JD035478

Zhang, J., Teng, Z., Huang, N., Guo, L., & Shao, Y. (2016). Surface renewal as a significant mechanism for dust emission. *Atmospheric Chemistry and Physics*, *16*(24), 15517–15528. https://doi.org/10.5194/acp-16-15517-2016

References From the Supporting Information

Gillette, D. A., Blifford, I. H., Jr., & Fenster, C. R. (1972). Measurements of aerosol size distributions and vertical fluxes of aerosols on land subject to wind erosion. *Journal of Applied Meteorology and Climatology*, *11*(6), 977–987. https://doi.org/10.1175/1520-0450(1972)011<0977:moasda>2.0.co;2

Ho, T. D., Valance, A., Dupont, P., & Ould El Moctar, A. (2011). Scaling laws in aeolian sand transport. *Physical Review Letters*, *106*(9), 094501. https://doi.org/10.1103/PhysRevLett.106.094501

Ishizuka, M., Mikami, M., Leys, J. F., Shao, Y., Yamada, Y., & Heidenreich, S. (2014). Power law relation between size-resolved vertical dust flux and friction velocity measured in a fallow wheat field. *Aeolian Research*, *12*, 87–99. https://doi.org/10.1016/j.aeolia.2013.11.002

Ju, T., Li, X., Zhang, H., Cai, X., & Song, Y. (2018). Comparison of two different dust emission mechanisms over the Horbin Sandy Land area: Aerosols contribution and size distributions. *Atmospheric Environment*, *176*, 82–90. https://doi.org/10.1016/j.atmosenv.2017.12.017

Kamath, S., Shao, Y., & Parteli, J. R. E. (2022). Scaling laws in Aeolian sand transport under low sand availability. *Geophysical Research Letters*, *49*(11), e2022GL097767. https://doi.org/10.1029/2022gl097767

Kamath, S. (2024). *A numerical model for aeolian sand transport and the concatenated dust emission*. Ph.D. thesis. University of Cologne.

Kawamura, R. (1964). Study of sand movement by wind. In *Hydraulic eng lab tech rep* (pp. 99–108). University of California.

Klose, M., Shao, Y., Li, X., Zhang, H., Ishizuka, M., Mikami, M., & Leys, J. F. (2014). Further development of a parameterization for convective turbulent dust emission and evaluation based on field observations. *Journal of Geophysical Research: Atmospheres*, *119*(17), 10441–10457. https://doi.org/10.1002/2014jd021688

Kok, J. F., Parteli, E. J. R., Michaels, T. I., & Karam, D. B. (2012). The physics of wind-blown sand and dust. *Reports on Progress in Physics*, *75*(10), 106901. https://doi.org/10.1088/0034-4885/75/10/106901

Li, X. L., Klose, M., Shao, Y., & Zhang, H. S. (2014). Convective turbulent dust emission (CTDE) observed over Horbin Sandy Land area and validation of a CTDE scheme. *Journal of Geophysical Research: Atmosheres*, *119*(16), 9980–9992. https://doi.org/10.1002/2014jd021572

Li, G., Zhang, J., Herrmann, H. J., Shao, Y., & Huang, N. (2020). Study of aerodynamic grain entrainment in aeolian transport. *Geophysical Research Letters*, *47*(11), e2019GL086574. https://doi.org/10.1029/2019GL086574

Liu, D., Ishizuka, M., Mikami, M., & Shao, Y. (2018). Turbulent characteristics of saltation and uncertainty of saltation model parameters. *Atmospheric Chemistry and Physics*, *18*(10), 7595–7606. https://doi.org/10.5194/acp-18-7595-2018

Mikami, M., Aoki, T., Ishizuka, M., Yabuki, S., Yamada, Y., Gao, W., & Zeng, F. (2005). Observation of number concentration of desert aerosols in the south of the Taklimakan Desert, China. *Journal of the Meteorological Society of Japan*, *83A*(0), 31–43. https://doi.org/10.2151/jmsj.83A.31

Owen, R. P. (1964). Saltation of uniform grains in air. *Journal of Fluid Mechanics*, *20*(2), 225–242. https://doi.org/10.1017/S0022112064001173

Raffaele, L., Bruno, L., Pellerey, F., & Preziosi, L. (2016). Windblown sand saltation: A statistical approach to fluid threshold shear velocity. *Aeolian Research*, *23*, 79–91. https://doi.org/10.1016/j.aeolia.2016.10.002

Shao, Y., Ishizuka, M., Mikami, M., & Leys, J. F. (2011). Parameterization of size-resolved dust emission and validation with measurements. *Journal of Geophysical Research*, *116*(D8), D08203. https://doi.org/10.1029/2010JD014527

Stout, J. E., & Zobeck, T. M. (1997). Intermittent saltation. *Sedimentology*, *44*(5), 959–970. https://doi.org/10.1046/j.1365-3091.1997.d01-55.x

White, B. R. (1979). Soil transport by winds on Mars. *Journal of Geophysical Research*, *84*(B9), 4643–4651. https://doi.org/10.1029/jb084ib09p04643

Yin, X., Jiang, C., Shao, Y., Huang, N., & Zhang, J. (2022). Large-eddy-simulation study on turbulent particle deposition and its dependence on atmospheric-boundary-layer stability. *Atmospheric Chemistry and Physics*, *22*(7), 4509–4522. https://doi.org/10.5194/acp-22-4509-2022

Zimon, A. D. (1982). *Adhesion of dust and powder*. Consultants Bureau.